

# Volume Preserving Threshold Dynamics for Grain Networks

Jing An

August 18, 2015

## Abstract

In this report, a volume preserving threshold dynamics is developed in order to simulate the grain networks in thin films of polycrystalline materials. This model maintains the spirit of the approximate energy proposed by Esedoglu and Otto, but with the volume preservation of air involved to simulate the surface grooving. Its algorithm and several programming results will be presented as well. Although adding the volume preservation provides stationary configurations, they are not stable, and we prove this instability in a simplified 2D case with two same-sized grains. In the end, we explore the basics of motion by surface diffusion, which is the correct way to simulate the surface grooving.

## 1 Introduction

### 1.1 Background

In material science, polycrystals refer to materials that are composed of many tiny single crystal pieces stuck together. These crystal pieces are named as *grains*, classified by misorientation angles. Polycrystalline materials exist in most ceramics and metals, and studying their grain boundary network is of great interest since some of their important physical properties, such as yield strength and conductivity, depend on it. When a thin film of a polycrystalline material is under annealing (heat treatment), its grain boundaries move. We are interested in simulating this evolution of grain networks and comparing it to the experimental results.

The inner grain boundary interfaces (in other words, 3D grain networks) follow motion by mean curvature. However, in 2D thin films, disagreements between the simulations based on curvature driven diffusion and experimental results arise in two aspects: 1. The stagnation of grain growth exists in experiments, while it does not happen in simulations. 2. In the statistical sense, the experimental samples have higher probabilities for smaller grains than the simulations do [2]. There are several possibilities trying to explain these discrepancies, and one of them is the surface grooving, a phenomenon that the free surface between air and film deforms. The goal of this project is to solve discrepancies using a modified model with the consideration of the surface grooving.

### 1.2 Mathematical Settings

Energy to describe the motion of grain boundaries in polycrystals when heat treated is as follows:

$$E(\Sigma_1, \dots, \Sigma_N) = \sum_{i \neq j}^N \sigma_{i,j} \text{Area}(\Gamma_{i,j}) = \sum_{i \neq j}^N \sigma_{i,j} \text{Area}(\partial \Sigma_i \cap \partial \Sigma_j) \quad (1)$$

Where  $\sigma_{i,j}$  is the *surface tension* associated with interface  $\Gamma_{i,j}$ .  $\sigma_{i,j} = \sigma_{j,i} > 0$  and  $\sigma_{i,j} = 0$  if  $i = j$ . To make the model well posed, it needs to satisfy the *triangle inequality*:

$$\sigma_{i,j} + \sigma_{j,k} \geq \sigma_{i,k}, \text{ for any } i, j \text{ and } k \quad (2)$$

The dynamics follow two important rules:

- At any point  $p \in \Gamma_{i,j} \setminus \mathcal{J}_{\geq 3}$  (here  $\mathcal{J}_{\geq 3}$  denotes junctions where more than three grains meet),  $\Gamma_{i,j}$  is smooth, then the normal speed is:

$$v_n(p) = \mu_{i,j} \sigma_{i,j} \kappa_{i,j}(p) \quad (3)$$

Where  $\kappa_{i,j} \geq 0$  is the mean curvature of  $\Gamma_{i,j}$ .  $\mu_{i,j}$  is the *mobility* associated with  $\Gamma_{i,j}$ . In this report, all mobilities are set to be 1.

- The triple junctions  $\mathcal{J}_3$  need to satisfy the Herring angle condition: At a junction formed by the meeting of the three phases  $\Sigma_1, \Sigma_2$  and  $\Sigma_3$ ,

$$\frac{\sigma_{1,2}}{\sin \theta_3} = \frac{\sigma_{1,3}}{\sin \theta_2} = \frac{\sigma_{2,3}}{\sin \theta_1} \quad (4)$$

Where  $\theta_i$  is the opening angle of the phase  $\Sigma_i$ .

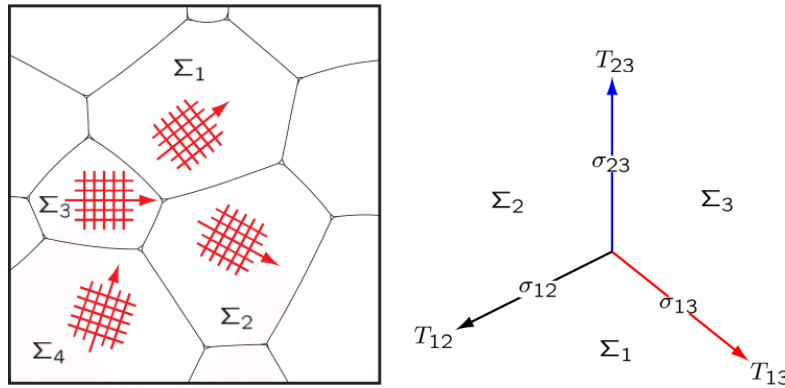


Figure 1: The left figure shows different grains classified by misorientation angles; the right figure is a triple junction where the Herring angle condition applies.

## 2 Previous Work

The motion by mean curvature equation well describes the inner grain interfaces, and its solution can be approximated by solving the Allen-Cahn equation [1]:

$$u_t = 2\varepsilon \Delta u - \frac{1}{\varepsilon} W'(u) \quad (5)$$

Which is the  $L^2$ -gradient descent of the Modica-Mortola Energy [8]:

$$E_\varepsilon(u) = \int \varepsilon |\nabla u|^2 + \frac{1}{\varepsilon} W(u) dx \quad (6)$$

Where  $W(\xi) : \mathbb{R} \rightarrow \mathbb{R}$  is a double well potential with equidepth wells at 0 and 1; for example,  $W(\xi) = \xi^2(1 - \xi)^2$ . The Modica-Mortola Energy approximates the perimeter of the object; it is composed of two parts: When  $\varepsilon \rightarrow 0^+$ , the second term forces  $u$  to behave like a characteristic function; the first part is the Dirichlet Energy, which penalizes the transitions between the object and the background, therefore measuring the object's boundary length.

## 2.1 MBO Scheme

Merriman, Bence and Osher [6] [7] introduced a threshold dynamics algorithm for motion by mean curvature. Their idea is to alternatively solve two parts of the equation (5). The first part is the diffusion equation which has a fundamental solution by convolving the propagator with the initial condition; the propagator is generally chosen to be the Gaussian kernel, which is positive, unit mass, radially symmetric ( $d$  is the dimension):

$$G_{\delta t}(x) = \frac{1}{(4\pi(\delta t))^{\frac{d}{2}}} e^{-\frac{|x|^2}{4(\delta t)}} \quad (7)$$

The second part is an ordinary differential equation, and it turns into *thresholding* when  $\varepsilon \rightarrow 0^+$ . Therefore, the threshold dynamics essentially is to alternate two steps, convolution and thresholding. The MBO scheme can be described as follows:

---

**MBO:** Given the partition  $\Sigma_1^k, \dots, \Sigma_N^k$  at time  $t = (\delta t)k$ , to get the partition  $\Sigma_1^{k+1}, \dots, \Sigma_N^{k+1}$  at the next time step  $t = (\delta t)(k+1)$ :

1. *Convolution step:*  $\phi_i^k = G_{\delta t} * \mathbb{1}_{\Sigma_i^k}$
  2. *Thresholding (redistribution) step:*  $\Sigma_i^{k+1} = \{x : \phi_i^k(x) > \phi_j^k(x) \text{ for all } j \neq i\}$
- 

This algorithm is unconditionally stable and very efficient: The convolution step can be done by the fast Fourier transform, and the thresholding step is trivial. Indeed, when surface tensions are equal ( $\sigma_{i,j} = 1$ , for  $i \neq j$ ), this threshold dynamics generates the gradient flow of energy (1). However, for arbitrary surface tensions, the MBO scheme is insufficient to satisfy the dynamics rules (3) and (4). It is true that (3) can be satisfied by modifying the thresholding step, but to achieve the correct Herring angle conditions (4) at junctions is more difficult.

## 2.2 The Approximate Energy

Recently, Esedoglu and Otto [5] introduced an approximation to the weighted surface area functional (1). The corresponding threshold dynamics-type scheme correctly generalizes to unequal surface tension with both conditions satisfied, and still maintains the spirit of the original MBO scheme.

The idea to approximate the surface area of the boundary  $\Gamma_{i,j}$  in (1) by the term:

$$\text{Area}(\Gamma_{i,j}) \approx \frac{1}{\sqrt{\delta t}} \int \mathbb{1}_{\Sigma_i} G_{\delta t} * \mathbb{1}_{\Sigma_j} dx \quad (8)$$

And therefore the approximate energy of (1) becomes:

$$E_{\delta t}(\Sigma_1, \dots, \Sigma_N) = \frac{1}{\sqrt{\delta t}} \sum_{i \neq j}^N \sigma_{i,j} \int \mathbb{1}_{\Sigma_i} G_{\delta t} * \mathbb{1}_{\Sigma_j} dx \quad (9)$$

The energy (9) can be relaxed by replacing the characteristic function set  $\{\mathbb{1}_{\Sigma_1}, \dots, \mathbb{1}_{\Sigma_N}\}$  by the admissible set  $\{u_1, \dots, u_N\}$ ,  $u_j(x) \in [0, 1]$  for all  $x$  and  $j$ . The relaxed energy has been proven to have the same minimization as the original approximate energy (9) does with the addition of a linear term [5]. Our proposed energy shown later is the extension of the following energy:

$$E_{\delta t}(u_1, \dots, u_N) = \frac{1}{\sqrt{\delta t}} \sum_{i \neq j}^N \sigma_{i,j} \int u_i G_{\delta t} * u_j dx, \text{ with } \sum_{i=1}^N u_i = 1 \text{ and } u_i \geq 0 \quad (10)$$

### 3 The Volume Preserving Energy

The minimization of the approximate energy (10) has successfully matches the experimental results in 3D grain networks. However, considering the free surface energy, this original approximate energy needs to be modified to simulate the surface grooving as well. The correct way to model the free surface boundaries is motion by surface diffusion, which is a fourth order partial differential equation,  $v_n = \Delta_S H_S$ . However, how to combine the motion by surface diffusion with threshold dynamics is challenging, and developing an efficient numerical scheme is considerably complicated. More related details will be discussed in section 6. Instead, here we will introduce a simple way to incorporate the free surface energy into the approximate energy (10). The idea is based on the physical fact that the total volume of the thin film stays constant. However, to preserve the total volume of grains is inefficient and not practicable. If we look at the thin film in a cubic computational domain, with the rest of space filled with air, we can view the air as an extra grain, say  $u_1$ , and preserve its volume  $V_1$  instead. Then we can get the follows:

$$E_{\delta t}(u_1, \dots, u_N) = \frac{1}{\sqrt{\delta t}} \int \sum_{i=1}^N [\sum_{j \neq i}^N \sigma_{i,j} G_{\delta t} * u_j(x)] u_i(x) dx + \lambda (\int u_1(x) dx - V_1),$$

$$\text{with } \sum_{i=1}^N u_i = 1 \text{ and } u_i \geq 0 \quad (11)$$

Where  $\lambda$  is a Lagrange multiplier. The energy can be rewritten as:

$$E_{\delta t} = \frac{1}{\sqrt{\delta t}} \int \underbrace{[\sum_{j \neq 1}^N \sigma_{1,j} G_{\delta t} * u_j(x) + \lambda \sqrt{\delta t}] u_1(x)}_{\text{weight 1}} + \dots + \underbrace{[\sum_{j \neq N}^N \sigma_{N,j} G_{\delta t} * u_j(x)] u_N(x)}_{\text{weight N}} dx - \lambda V_1 \quad (12)$$

The idea to minimize  $E_{\delta t}$  is similar to minimizing the energy (10): At each position  $x$ , we assign all the unit mass to the region where it has the smallest weight. This redistribution ensures the total energy will not increase at each time step given computed weights. The motion of internal grain boundaries still follow (3), but the normal speed of the free grain surface, corresponding to this revised energy, becomes  $v_n = H - \lambda(t)$ , where  $H$  is the mean curvature of the free surface.

Different from the previous minimization, in each iteration, we need an extra step for finding the correct  $\lambda$ . At time  $t = (\delta t)n$ , with an initial guess  $\lambda_0^{(n)}$ , we can get a sequence  $\{\lambda_k^{(n)}\}_{k \geq 0}$  by:

$$\lambda_{k+1}^{(n)} = \lambda_k^{(n)} - \varepsilon (V_1 - \int u_1^{(n+1),k}(x) dx) \quad (13)$$

Where  $\varepsilon > 0$  is a constant time difference. When  $V_1 > \int u_1^{(n+1),k}(x) dx$ , it implies weight 1 is too large to include more points, so  $\lambda^{(n)}$  needs to be smaller; when  $V_1 < \int u_1^{(n+1),k}(x) dx$ , it implies weight 1 includes

too many points, so  $\lambda^{(n)}$  needs to be larger to increase weight 1; when  $V_1 = \int u_1^{(n+1),k}(x)dx$ ,  $\lambda_{k+1}^{(n)} = \lambda_k^{(n)}$ , the sequence converges. This convergence within tolerance error can be quickly found by the bisection method.

Our algorithm is the analogue of the standard MBO scheme, with an intermediate step of updating  $\lambda$  involved. A complete description of the algorithm is as follows:

---

**Algorithm:** Given the partition  $\Sigma_1^k, \dots, \Sigma_N^k$  at time  $t = (\delta t)k$ , to get the partition  $\Sigma_1^{k+1}, \dots, \Sigma_N^{k+1}$  at the next time step  $t = (\delta t)(k+1)$ :

1. *Convolution step:* To get the sum of weighted convolutions, we first compute the approximate characteristic functions  $u_i^k$  to replace  $\mathbb{1}_{\Sigma_i^k}$ , then:

$$\phi_i^k = \sum_{j=1}^N \sigma_{i,j} G_{\delta t} * u_j^k \quad (14)$$

2. *Thresholding step:*

$$\Sigma_i^{k+1} = \{x : \phi_i^k(x) < \min_{j \neq i} \phi_j^k(x)\} \quad (15)$$

3. Find  $\lambda^k$  based on  $u_j^{k+1}$ .
  4. Revise  $\phi_1^k = \phi_1^k + \lambda$ , apply the thresholding step again.
- 

(15) can be replaced by a level set function to delineate the boundary of grain  $i$  at the end of time step  $k$ :

$$\psi_i^{k+1}(x) = \min_{l \neq i} \phi_l^k(x) - \phi_i^k(x) \quad (16)$$

Then we have:

$$\Sigma_i^{k+1} = \{x : \psi_i^{k+1} > 0\} \quad (17)$$

For equal surface tensions  $\sigma$ , the new algorithm reduces to the original MBO scheme. Because at time  $t = (\delta t)k$ , weight  $i$  for point  $x = \sigma(\sum_{j=1}^N G_{\delta t} * u_j^k(x) - G_{\delta t} * u_i^k(x)) = \sigma(G_{\delta t} * \sum_{j=1}^N u_j^k(x) - G_{\delta t} * u_i^k(x)) = \sigma(G_{\delta t} * 1 - G_{\delta t} * u_i^k(x))$ . The algorithm can be much more efficient by looking at:

$$\phi_i^k = G_{\delta t} * u_i^k(x)$$

And we define the level set function to be:

$$\psi_i^{k+1}(x) = \phi_i^k(x) - \max_{l \neq i} \phi_l^k(x)$$

## 4 Result

### 4.1 Rate of Convergence

In this section, we analyze the convergence of the algorithm for volume preserving curvature motion. The initial condition for the test is a 2D configuration with air and two same-sized grains of the height 1/2

(shown in Figure 2). The computational domain is  $[0, 1] \times [0, 1]$ , and the surface tensions are equal ( $\sigma = 1$ ).

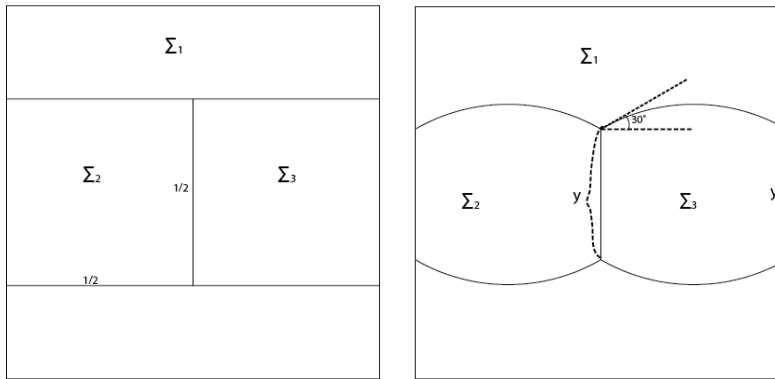


Figure 2: The left figure is the initial condition, the right one is the configuration after evolution. Here the exact  $y$  is  $\frac{1}{2} + \frac{\sqrt{3}}{4} - \frac{\pi}{6}$

The rate of convergence can be computed in  $\log\left(\frac{u_h - u^*}{u_{h/2} - u^*}\right)$ , where  $u^*$  is the exact value, and  $u_h$  and  $u_{h/2}$  are values obtained from simulations with step sizes  $h$  and  $h/2$  respectively. Here we measure the grain interface length (vertical line in figure), and  $u^* = \frac{1}{2} + \frac{\sqrt{3}}{4} - \frac{\pi}{6} \approx 0.4094139$ . The error in the interface length and its associated convergence rate are displayed in the table below:

Table 1: Convergence of Algorithm

Resolution	Step Size	Length	Error	Order
$64 \times 64$	0.0176	28/64	0.028	—
$128 \times 128$	0.0088	54/128	0.01246	1.17
$256 \times 256$	0.0044	106/256	0.00465	1.422
$512 \times 512$	0.0022	212/512	0.00465	0
$1024 \times 1024$	0.0011	422/1024	0.002695	0.787
$2048 \times 2048$	0.00055	842/2048	0.001718	0.65

The expected convergence rate is  $1/2$ . We noticed that for the resolution  $512 \times 512$ , its convergence rate stagnates compared to the previous one, but it is not unreasonable: Since the first several resolutions have pretty fast convergence, it stagnates in the middle, then regains its order. The latter ones are slower than before, and get closer to the expected rate  $1/2$ .

## 4.2 Grain Sizes Distribution

In this section, we statistically study the grain sizes distribution in the time evolution. The computational domain is still  $[0, 1] \times [0, 1]$  with grid sizes  $256 \times 256$ . The test started with 400 grains constructed by voronoi diagram, grains' total volume is  $11/32$  and all surface tensions are equal ( $=1$ ). We chose a proper  $dt$  by testing the motion by mean curvature of the 3D sphere. Since for a 3D sphere, the change rate of its radii follows the ODE:  $\frac{d}{dt}r(t) = H = -\frac{2}{r}$ . Then its solution is  $r(t) = \sqrt{r(0)^2 - 4t}$ . We began with  $r(0) = 1/4$ , then when  $r(t) = 1/8$ , the exact  $t$  should be  $3/256$ . In grid sizes  $256 \times 256$ , we found  $dt = 0.00024$  ensured

that the required time  $t$  to get  $r(t) = 1/8$  can be within error  $< 5\%$ .

Figure 3 gives the result when 92 grains remain after  $t = 0.00504$ . The first two pictures from different angles of view show the distribution of these grains. And the picture below is a statistical diagram:  $A$  refers to the area of the grain, and  $\langle A \rangle$  is the average area  $= 1/92$ . Each point corresponds to the number of grains having the value  $A/\langle A \rangle$  stay in  $(\frac{i-1}{10}, \frac{i}{10}]$ ,  $i = 1, 2, \dots, 28$ .

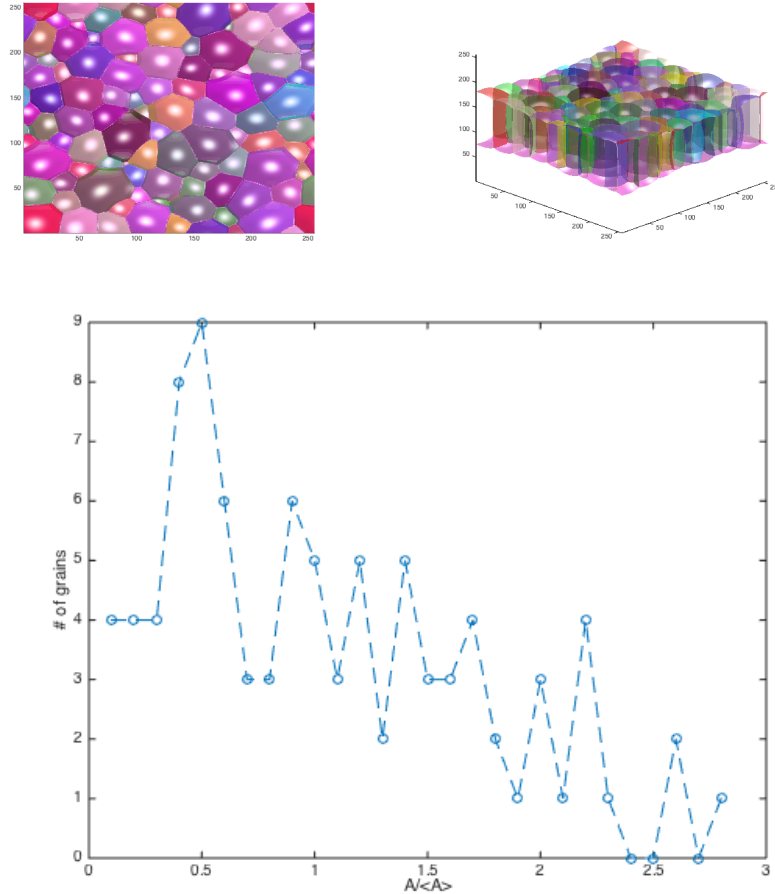


Figure 3: Equal surface tensions  $\sigma = 1$ . At  $t = 0.00504$ , 92 remaining grains from the dynamics starting with 400 grains.

### 4.3 Stagnation

We are also interested in investigating if the volume preserving threshold dynamics will present the stagnation as the experiments have. The following figures show the evolution of grains under volume preserving curvature motion. In both cases, the surface tensions between grains are 1, but the air-grain surface tension varies. The tests start with 100 grains in the same computational domain as before, and the grid sizes are  $128 \times 128$ .  $dt = 0.00024$ .

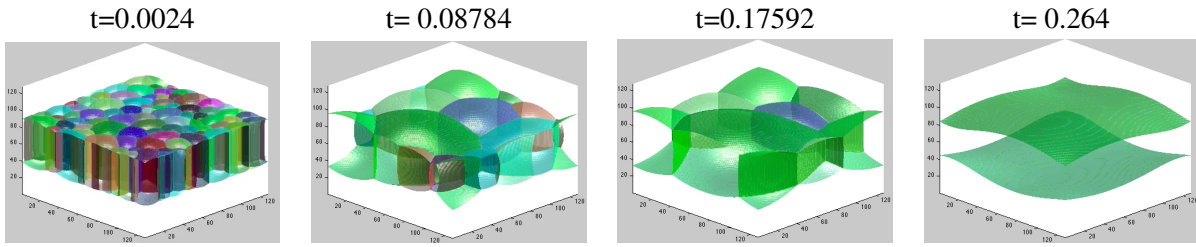


Figure 4: Air-grain surface tension  $\sigma = 1$

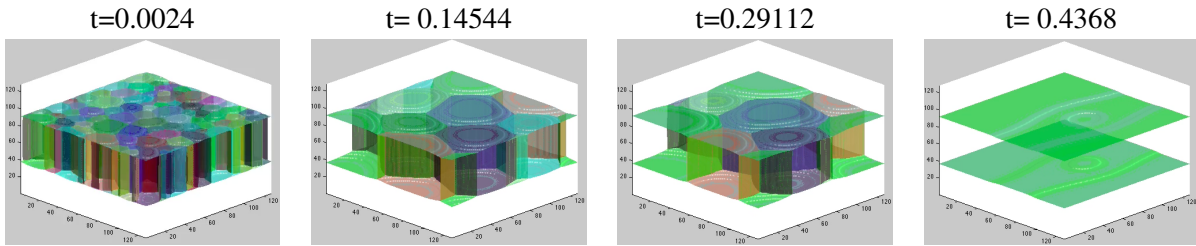


Figure 5: Air-grain surface tension  $\sigma = 2$

With larger  $\sigma$ , we can see the free surfaces deform less, and it requires more time to let 100 grains reduce to be one (or two) grain.

Indeed, no matter what air-grain surface tensions  $\sigma$  we choose, the simulations do not stagnate. But it is necessary to include the volume preservation term, otherwise the free surfaces will travel towards each other and pinch off the film; however, even though volume preservation introduces stationary configurations, they are not stable, therefore not explaining stagnation. The next section will discuss more about its instability.

## 5 Proof of Instability

In this section, we will show a simple proof of instability of the stationary configuration from volume preserving threshold dynamics. We look into a 2D configuration with two same-sized grains of the height  $h$ , and its computational domain is  $[0, 1] \times [0, 1]$ . The surface tension between two grains are 1, and the air-grain surface tension is  $\sigma$ . After the evolution driven by our proposed algorithm, the stationary configuration is shown as in Figure 6.

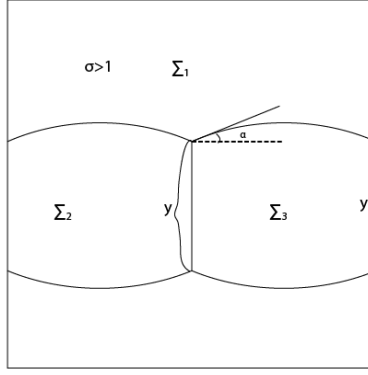


Figure 6: Stationary configuration with air-grain surface tension  $\sigma > 1$

Notice that the energy we analyze here is  $E(\Sigma_1, \Sigma_2, \Sigma_3) = \sigma \text{Per}(\Gamma_{13}) + \sigma \text{Per}(\Gamma_{12}) + \text{Per}(\Gamma_{23})$ , then we introduce the following conjecture:

**Conjecture 5.1.** *The configuration Figure 6 is unstable: We can find any configuration in its neighborhood has strictly less surface energy.*

*Proof.* First of all, by triangle inequality,  $\sigma \in (\frac{1}{2}, \infty)$ . Herring angle condition  $\frac{\sigma_{12}}{\sin(\pi/2+\alpha)} = \frac{\sigma_{13}}{\sin(\pi/2+\alpha)} = \frac{\sigma_{23}}{\sin(\pi-2\alpha)}$  gives that

$$\sigma = \sigma_{1k} = \frac{1}{2 \sin \alpha}, k = 2, 3 \quad (18)$$

By Figure 6,  $4r_0 \sin \alpha = 1 \Rightarrow r_0 = \frac{\sigma}{2}$ .

$$\begin{aligned} y + \sigma^2 \left( \alpha - \frac{\sin 2\alpha}{2} \right) &= h \\ \Rightarrow y &= h - \sigma^2 \left( \alpha - \frac{\sin 2\alpha}{2} \right) \end{aligned} \quad (19)$$

Therefore,

$$E_1 = 2y + \sigma \cdot (\text{Arclength}(\Gamma_{12}) + \text{Arclength}(\Gamma_{13})) = 2y + 4\sigma^2 \alpha = 2h - 2\alpha \sigma^2 + \sigma \cos \alpha + 4\sigma^2 \alpha \quad (20)$$

Then we compute the energy for the case with perturbation  $\Delta x$ , as shown in Figure 7. Because we just analyze the configurations in the small neighborhood of Figure 6, we can assume that the interfaces between 2 grains are still straight, and the angle of  $\Gamma_{12}, \Gamma_{13}$  is closed to  $\pi - 2\alpha$ , so the angle difference can be neglected.

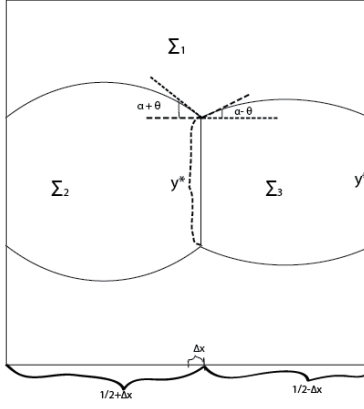


Figure 7: Perturbed configuration

Because of  $v_n = \kappa - \lambda$ , when the moving boundaries stop,  $\kappa = \nabla \left( \frac{\nabla \phi}{|\nabla \phi|} \right) = \frac{1}{r} \equiv \lambda$ . So the radii  $r$  for  $\Sigma_2$  and  $\Sigma_3$  are equal.

$r, \theta, \Delta x$  are unknowns, but we can get their relationships by the following observations:  
First of all, the sum of horizontal lengths preserves:

$$\begin{aligned} 2r \sin(\alpha - \theta) + 2r \sin(\alpha + \theta) &= 1 \\ \Rightarrow 4r \sin \alpha \cos \theta &= 1 \end{aligned} \quad (21)$$

Secondly, the difference of two horizontal lengths is  $2\Delta x$ :

$$\begin{aligned} 2r \sin(\alpha + \theta) - 2r \sin(\alpha - \theta) &= 2\Delta x \\ \Rightarrow 2r \cos \alpha \sin \theta &= \Delta x \end{aligned} \quad (22)$$

By  $\cos^2 \theta + \sin^2 \theta = 1$ , we then have the relationship

$$r^2 = \frac{\sigma^2}{4} + \frac{\Delta x^2}{4 - 1/\sigma^2} \quad (23)$$

We can also get new  $y^*$  by computing the preserved area:

$$\begin{aligned} y^* + 1 - h + 2 \left[ \pi r^2 \frac{2\alpha + 2\theta}{2\pi} - r^2 \sin(\alpha + \theta) \cos(\alpha + \theta) \right] \\ + 2 \left[ \pi r^2 \frac{2\alpha - 2\theta}{2\pi} - r^2 \sin(\alpha - \theta) \cos(\alpha - \theta) \right] &= 1 \\ \Rightarrow y^* &= h + 2r^2 \sin 2\alpha \cos 2\theta - 4r^2 \alpha \end{aligned} \quad (24)$$

Plug (24) in, we obtain the energy for the perturbed configuration:

$$\begin{aligned} E_2 &= 2y^* + \sigma \cdot (\text{Arclength}(\Gamma_{12}) + \text{Arclength}(\Gamma_{13})) = 2y^* + 8r\alpha\sigma \\ &= 2h + 4r^2 \sin 2\alpha \cos 2\theta - 8r^2 \alpha + 8r\alpha\sigma \end{aligned} \quad (25)$$

$$\Delta E = E_2 - E_1 = -4(\sin 2\alpha + 2\alpha)r^2 + 8\alpha\sigma r + (\sigma \cos \alpha + 2\alpha\sigma^2 - 4\sigma^2\alpha) \quad (26)$$

$r = \sigma/2$  is the root of  $\Delta E$ , and the axis of symmetry is located at  $r = \frac{\alpha\sigma}{\sin 2\alpha + 2\alpha}$ , where  $\Delta E$  obtains the maximum value. To show that  $\Delta E < 0$ , we notice that as long as  $\Delta x \neq 0, r > \sigma/2$ ; if  $\Delta E$  is monotonically decreasing on  $[\sigma/2, +\infty)$ , then  $\Delta E < 0$ .

Indeed, (23) can be rewritten as  $\Delta x^2 = (4 - 1/\sigma^2) \cdot (r^2 - \sigma^2/4)$ . Since  $\sigma > 1/2$ , the first component is always positive. So as long as  $\Delta x \neq 0, \Delta x^2 > 0$ , then  $r$  must be larger than  $\sigma/2$ . To show that  $\Delta E$  is monotonically decreasing on  $[\sigma/2, +\infty)$ , we just need to show that the root  $r = \sigma/2$  is always on the right hand side of the axis of symmetry:

$$\frac{\alpha\sigma}{\sin 2\alpha + 2\alpha} - \frac{\sigma}{2} = \frac{\sigma}{2} \left( \frac{\alpha}{\frac{\sin 2\alpha}{2} + \alpha} - 1 \right) < 0$$

Because  $\alpha \in (0, \frac{\pi}{2})$ ,  $\frac{\sin 2\alpha}{2} > 0$ . Therefore,  $\frac{\alpha\sigma}{\sin 2\alpha + 2\alpha} < \frac{\sigma}{2}$  for  $\forall \alpha \in (0, \frac{\pi}{2})$ . Therefore, for all air-surface tensions, we can always find configurations in the neighborhood of Figure 6 having strictly less energy. Since this simple 2D case is representative and can be generalized into 3D, we conclude that the stationary configurations introduced by the volume preserving threshold dynamics are unstable with any air-grain surface tensions.

**Comment:**  $\frac{d^2}{dr^2}(\Delta E) = -8(\sin 2\alpha + 2\alpha)$ . When  $\sigma$  is very large, then by (18)  $\alpha$  is correspondingly very small, which implies that the change of speed is slow, i.e., the deformation is relatively trivial. Therefore, the energy difference will be close to zero even though we apply nontrivial perturbations.

## 6 Motion by Surface Diffusion

Surface diffusion is an important grain growth mechanism in material science. To correctly describe the surface grooving, we look at motion by surface diffusion:

$$v_n = \Delta_S H_S \tag{27}$$

Where  $\Delta_S$  is the surface Laplacian (or Laplace-Beltrami operator) for the parametrized surface  $S$ .

The motion by surface diffusion has two important properties:

- *Area-decreasing:* Let  $A(t)$  denote the area of  $S(t)$  at time  $t$ ,

$$\begin{aligned} \frac{1}{2} \frac{d}{dt} A(t) &= \int_{S(t)} v_N H_{S(t)} d\sigma = \int_{S(t)} (\Delta_{S(t)} H_{S(t)}) H_{S(t)} d\sigma \\ &= - \int_{S(t)} (\nabla_{S(t)} H_{S(t)})^2 d\sigma \leq 0 \end{aligned} \tag{28}$$

- *Volume-preserving:* Let  $\text{Vol}(t)$  denote the volume bounded by  $S(t)$  at time  $t$ ,

$$\frac{d}{dt} \text{Vol}(t) = \int_{S(t)} v_N d\sigma = \int_{S(t)} \Delta_{S(t)} H_{S(t)} d\sigma = 0 \tag{29}$$

And these two properties motivate us to replace the volume preserving curvature driven flow for the air ( $\Sigma_1$ ) by the surface diffusion driven flow.

## 6.1 Degenerated Cahn-Hilliard Equation

Recall the perimeter approximation energy (6) we mentioned in the section 2:

$$E_\varepsilon(u) = \int \varepsilon |\nabla u|^2 + \frac{1}{\varepsilon} W(u) dx \quad (30)$$

Consider the perturbation of  $u(x)$ , and we take derivative of perturbed energy in terms of time  $t$ :

$$\begin{aligned} \frac{d}{dt} E_\varepsilon(u + t\phi)|_{t=0} &= \frac{d}{dt} \int \varepsilon |\nabla u + t\nabla\phi|^2 + \frac{1}{\varepsilon} W(u + t\phi) dx \\ &= \int [-2\varepsilon\Delta u + \frac{1}{\varepsilon} W'(u)]\phi dx = \langle \nabla_u E, \phi \rangle_{H^{-1}} \end{aligned}$$

Here, the  $H^{-1}$  inner product is defined as  $\langle f, g \rangle_{H^{-1}} = -\int f \Delta^{-1} g dx$ . Therefore, the  $H^{-1}$  gradient descent of  $E_\varepsilon$  is:

$$u_t = -\nabla_u E = -\Delta[2\varepsilon\Delta u - \frac{1}{\varepsilon} W'(u)] \quad (31)$$

Which is the Cahn-Hilliard equation [3], solving this phase field model can simulate the surface diffusion. This motion can be generated by solving a sequence of variational problems, known as the minimizing movements approach. At  $n$ th time step:

$$u^{n+1}(x) = \operatorname{argmin}_u E_\varepsilon(u) + \frac{1}{\delta t} \|u - u^n\|_{H^{-1}}^2 \quad (32)$$

The second term is a ‘‘movement limiter’’ preventing the updated step from getting too far from the current step.

We want to measure the boundary of  $u$  in  $H^{-1}$  norm. However, rather than bother parametrizing the boundary, we can involve a mobility term (e.g.  $u(1-u)$ ) to help us focus on  $u$ 's boundary only. So the  $H^{-1}$  gradient descent of (32) is:

$$u_t = -\nabla \cdot (u(1-u)\nabla(2\varepsilon\Delta u - \frac{1}{\varepsilon} W'(u))) \quad (33)$$

Which we call the Cahn-Hilliard equation with degenerate mobility. Solving this fourth order PDE can help us simulate the motion by surface diffusion.

## 6.2 Finite Difference for Motion by Surface Diffusion

Our future goal is to incorporate the degenerated Cahn-Hilliard equation into the variational formulation of threshold dynamics for grain growth. However, due to the time limit, I only studied the finite difference for motion by surface diffusion in 1D and 2D during the REU program.

Part I (1D): To find the motion by surface diffusion equation for  $f(x, t)$ , we look at its level set function:

$$\phi(x, y, t) = y - f(x, t) \quad (34)$$

The equation of motion of the level set function for surface diffusion is:

$$\phi_t = -|\nabla\phi|v_n \Rightarrow f_t = \sqrt{1 + f_x^2} v_n \quad (35)$$

Where  $v_n = \partial_S^2 \kappa(x)$ . As  $S(x) = \int_0^x \sqrt{1 + f'(\xi)^2} d\xi$ ,  $\frac{dS}{dx} = \sqrt{1 + f'(x)^2}$ . And by change of variables,  $\frac{d\kappa}{dS} = \frac{d}{dx} \kappa / \frac{dS}{dx}$ , we finally get the formula:

$$f_t = -\frac{\partial}{\partial x} \left( \frac{1}{\sqrt{1 + f_x^2}} \frac{\partial}{\partial x} \left( \frac{\partial}{\partial x} \left( \frac{f_x}{\sqrt{1 + f_x^2}} \right) \right) \right) \quad (36)$$

And we choose the discretization of this fourth order PDE to be:

$$f_t = -D^- \left( \frac{1}{\sqrt{1 + (D^+ f)^2}} D^+ \left( D^- \left( \frac{D^+ f}{\sqrt{1 + (D^+ f)^2}} \right) \right) \right) \quad (37)$$

Here,  $D^+$  refers to the Forward Euler, and  $D^-$  refers to the Backward Euler.

Part II (2D): To find the motion by surface diffusion equation for  $f(x, y, t)$ , we look at its level set function:

$$\phi(x, y, z, t) = z - f(x, y, t) \quad (38)$$

Since  $H = \nabla \cdot \left( \frac{\nabla \phi}{|\nabla \phi|} \right)$ , we get:

$$H = -\frac{f_{xx} + f_{yy}}{\sqrt{1 + f_x^2 + f_y^2}} + \frac{f_x^2 f_{xx} + 2f_x f_y f_{xy} + f_y^2 f_{yy}}{(1 + f_x^2 + f_y^2)^{\frac{3}{2}}} \quad (39)$$

According to [9],  $\nabla_S H = \nabla H - \vec{n} \partial_{\vec{n}} H$ , where  $\partial_{\vec{n}} = \vec{n} \cdot \nabla H = n_x H_x + n_y H_y$ , with

$$n_x = \frac{f_x}{\sqrt{1 + f_x^2 + f_y^2}}, n_y = \frac{f_y}{\sqrt{1 + f_x^2 + f_y^2}} \quad (40)$$

As  $\Delta_S = \nabla_S \cdot \nabla_S$ , with several computations, we finally get:

$$f_t = \Delta_S H_S = A_x + B_y - n_x (A_x n_x + A_y + n_y) - n_y (B_x n_x + B_y n_y) \quad (41)$$

With

$$A = H_x - f_x \left( \frac{f_x H_x + f_y H_y}{1 + f_x^2 + f_y^2} \right), B = H_y - f_y \left( \frac{f_x H_x + f_y H_y}{1 + f_x^2 + f_y^2} \right)$$

The finite difference for (41) is the same as in Part I, that is alternatively applying Forward and Backward Euler, and the innermost part  $f_x$  starts with Forward Euler.

Time steps for both 1D and 2D cases are heavily limited by the CFL condition [4]. Better numerical methods have been discussed in many papers, for example, semi-implicit method [9]. However, There is still much space to get improved, especially for the surface diffusion with degenerated mobility, which is nonlinear and therefore much more complicated to implement.

## 7 Conclusion

We have presented the volume preserving threshold dynamics and its algorithm. Relative numerical analysis and simulated results have been shown as well. In the future, we will focus on incorporating the Cahn-Hilliard equation with degenerate mobility into the variational formulation of threshold dynamics to better simulate grain networks. It also requires much work including developing an efficient numerical scheme, which is very challenging.

## 8 Acknowledgment

I would like to thank Professor Selim Esedoglu for his guidance and generous financial support. I would also like to thank the technology support from University of Michigan, and Department of Mathematics for organizing the REU program.

## References

- [1] Samuel Miller Allen and John W Cahn. Ground state structures in ordered binary alloys with second neighbor interactions. *Acta Metallurgica*, 20(3):423–433, 1972.
- [2] K Barmak, J Kim, C-S Kim, WE Archibald, GS Rohrer, AD Rollett, D Kinderlehrer, S TaAsan, H Zhang, and DJ Srolovitz. Grain boundary energy and grain growth in al films: Comparison of experiments and simulations. *Scripta materialia*, 54(6):1059–1063, 2006.
- [3] John W Cahn and John E Hilliard. Free energy of a nonuniform system. i. interfacial free energy. *The Journal of chemical physics*, 28(2):258–267, 1958.
- [4] Richard Courant, Kurt Friedrichs, and Hans Lewy. Über die partiellen differenzengleichungen der mathematischen physik. *Mathematische Annalen*, 100(1):32–74, 1928.
- [5] Selim Esedoglu and Felix Otto. Threshold dynamics for networks with arbitrary surface tensions. *Communications on Pure and Applied Mathematics*, 68(5):808–864, 2015.
- [6] Barry Merriman, James K Bence, and Stanley J Osher. Motion of multiple junctions: A level set approach. *Journal of Computational Physics*, 112(2):334–363, 1994.
- [7] Barry Merriman, James Kenyard Bence, and Stanley Osher. *Diffusion generated motion by mean curvature*. Proceedings of the Computational Crystal Growers Workshop, 1992.
- [8] Luciano Modica and Stefano Mortola. Un esempio di  $\gamma$ -convergenza. *Boll. Un. Mat. Ital. B (5)*, 14(1):285–299, 1977.
- [9] Peter Smereka. Semi-implicit level set methods for curvature and surface diffusion motion. *Journal of Scientific Computing*, 19(1):439–456, 2003.